

## Spectroscopic Determination of an Anion-# Bond Strength

Cate S. Anstöter, Joshua P. Rogers, and Jan R. R. Verlet

*J. Am. Chem. Soc.*, **Just Accepted Manuscript** • DOI: 10.1021/jacs.9b01345 • Publication Date (Web): 02 Apr 2019

Downloaded from <http://pubs.acs.org> on April 3, 2019

### Just Accepted

“Just Accepted” manuscripts have been peer-reviewed and accepted for publication. They are posted online prior to technical editing, formatting for publication and author proofing. The American Chemical Society provides “Just Accepted” as a service to the research community to expedite the dissemination of scientific material as soon as possible after acceptance. “Just Accepted” manuscripts appear in full in PDF format accompanied by an HTML abstract. “Just Accepted” manuscripts have been fully peer reviewed, but should not be considered the official version of record. They are citable by the Digital Object Identifier (DOI®). “Just Accepted” is an optional service offered to authors. Therefore, the “Just Accepted” Web site may not include all articles that will be published in the journal. After a manuscript is technically edited and formatted, it will be removed from the “Just Accepted” Web site and published as an ASAP article. Note that technical editing may introduce minor changes to the manuscript text and/or graphics which could affect content, and all legal disclaimers and ethical guidelines that apply to the journal pertain. ACS cannot be held responsible for errors or consequences arising from the use of information contained in these “Just Accepted” manuscripts.

# Spectroscopic Determination of an Anion- $\pi$ Bond Strength

Cate S. Anstöter, Joshua P. Rogers, Jan R. R. Verlet\*

Department of Chemistry, Durham University, Durham DH1 3LE, United Kingdom

Supporting Information Placeholder

**ABSTRACT:** The anion- $\pi$  bond has emerged as an important non-valence interaction in supramolecular and biological structure. Although recognized as a strong non-covalent interaction, driven by electrostatic charge-quadrupole moment and correlation interactions, benchmark experimental and computational studies on the intrinsic anion- $\pi$  bond strength are scarce. Here, we present a gas-phase photoelectron spectroscopic study on the archetypical iodide-hexafluorobenzene anion- $\pi$  bonded complex. In combination with high-level electronic structure calculations, the anion- $\pi$  bond strength is found to be 0.53 eV (51 kJ mol<sup>-1</sup>). The interaction arises for a large part from correlation forces (~40%), with electrostatic quadrupole-anion and polarization making up most of the remainder.

Noncovalent interactions are a deterministic component of macromolecular and condensed phase structure. They include bonds such as hydrogen bonds, halogen bonds,  $\pi$ - $\pi$  stacking interactions, and cation- $\pi$  bonds.<sup>1-6</sup> The full exploitation of noncovalent bonds in chemical design and reactivity is underpinned by a basic physical understanding of such interactions, much of which has been built upon careful spectroscopic measurements on isolated (gas phase) systems that serve as benchmarks for theoretical models. A relatively new addition to the family of noncovalent interactions is the anion- $\pi$  bond. First predicted theoretically,<sup>7-9</sup> the interaction arises between an electron deficient  $\pi$ -system and an anion. The anion- $\pi$  bond is now recognized and exploited as a key interaction in anion-recognition and supramolecular chemistry.<sup>10-20</sup> However, while the exploitation of anion- $\pi$  bonds is a rapidly growing field, the basic chemical physics of the interaction is not fully developed, which is in large part due to the lack of direct spectroscopic data on the anion- $\pi$  bond.<sup>14,21</sup> Here, we fill this void by using photoelectron spectroscopy in combination with electronic structure calculations to determine the interaction strength of the archetypical anion- $\pi$  bonded complex, iodide-hexafluorobenzene ( $\Gamma$ -C<sub>6</sub>F<sub>6</sub>).

Cation- $\pi$  bonds arise from the electrostatic quadrupole-charge interaction of an electron rich  $\pi$ -system with a cation.<sup>22,23</sup> The electrostatic attraction between an anion and a  $\pi$ -system can be achieved by the addition of electron-withdrawing substituents that lead to a positive quadrupole moment along the axis perpendicular to the  $\pi$ -system,  $Q_{zz}$ .<sup>24</sup> As in the case of the cation- $\pi$  bond, correlation forces play an important role.<sup>25</sup> However, quantitative analysis of the relative importance of these forces requires experimental data that is devoid of other interactions. Isolated anion- $\pi$  complexes have been studied by mass spectrometry,<sup>12,26</sup> providing qualitative information. Recently, Wang and coworkers performed photoelectron spectroscopy on a series of anions complexed to the  $\pi$ -system, tetraoxacalix[2]arene[2]triazine.<sup>27</sup> This revealed a large increase in the anion's electron binding energy when complexed, indicating that a strong cohesion energy between the two. However, a detailed analysis of the bond strength was not attempted. Here, such an

analysis is provided on  $\Gamma$ -C<sub>6</sub>F<sub>6</sub>, which was chosen not only as a benchmark anion- $\pi$  bonded complex, but also because it is free from any other noncovalent interactions.

Experimentally,  $\Gamma$  was condensed onto C<sub>6</sub>F<sub>6</sub> using a molecular beam source.<sup>28,29</sup> A mixture of CF<sub>3</sub>I and Ar (4 bar) was passed over liquid C<sub>6</sub>F<sub>6</sub> and expanded into vacuum through a pulsed valve. The resultant expansion was crossed by an electron beam forming  $\Gamma$  by dissociative electron attachment to CF<sub>3</sub>I, which subsequently clustered to C<sub>6</sub>F<sub>6</sub> in the supersonic expansion to form  $\Gamma$ -C<sub>6</sub>F<sub>6</sub>. The  $\Gamma$ -C<sub>6</sub>F<sub>6</sub> complexes were mass-selected by time-of-flight and intersected with light from a tunable Nd:YAG pumped OPO. Resultant photoelectrons were analyzed using a velocity map imaging spectrometer,<sup>30,31</sup> which was calibrated to the photoelectron spectrum of  $\Gamma$ . The molecular beam source ensures that the complex is cold (on the order of 10s K).

The  $\Gamma$ -C<sub>6</sub>F<sub>6</sub> complex was also treated computationally using equation-of-motion coupled cluster theory EOM-IP-CCSD(dT) with the Dunning aug-cc-pVDZ basis set.<sup>32,33</sup> The complex was optimized and verified to be the minimum energy structure by vibrational analysis. All calculations employed the frozen-core approximation and were carried out using the QChem 5.0 computational package.<sup>34</sup> A rigid potential energy scan was calculated at this level of theory by changing the distance between the  $\Gamma$  and the center of the C<sub>6</sub>F<sub>6</sub> ring. Additionally, an energy decomposition analysis (EDA) based on absolutely localized molecular orbitals (ALMO)<sup>35</sup> was performed to determine the contributions to the self-consistent field (SCF) energy of the complex.

Figure 1 shows the photoelectron spectra of  $\Gamma$  and  $\Gamma$ -C<sub>6</sub>F<sub>6</sub> taken with photon energy of 4.40 and 4.80 eV, respectively, so that both peaks have similar electron kinetic energies. The spectra are plotted in electron binding energy (eBE = photon energy minus electron kinetic energy) and clearly show that there is a blue-shift in the eBE of  $\Gamma$ -C<sub>6</sub>F<sub>6</sub> relative to  $\Gamma$ . From Figure 1, this shift,  $\Delta$ eBE = 0.42  $\pm$  0.02 eV. Additionally, both spectra have essentially the same spectral profile.

The similarity between the  $\Gamma$  and  $\Gamma$ -C<sub>6</sub>F<sub>6</sub> spectra suggest that the charge is predominantly located on the iodide with the C<sub>6</sub>F<sub>6</sub> simply solvating this anion.<sup>28</sup> Therefore, to a first approximation,  $\Delta$ eBE can be assigned to the cohesion energy of the anionic complex – *i.e.* the anion- $\pi$  bond. However, this ignores the final (neutral) state, where the I-C<sub>6</sub>F<sub>6</sub> interaction is not negligible. Hence, *ab-initio* electronic structure calculations are essential to also assess neutral potential energy surface (PES) and to determine an accurate anion- $\pi$  bond strength.

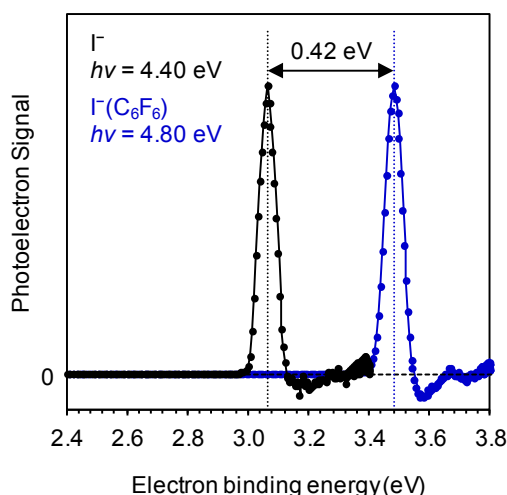


Figure 1: Photoelectron spectra of  $\text{I}^-$  and  $\text{I}^-\text{C}_6\text{F}_6$  taken at 4.40 and 4.80 eV, respectively. The vertical dashed lines indicate the peak positions, which are separated by 0.42 eV.

Figure 2(a) shows the minimum energy geometry of the  $\text{I}^-\text{C}_6\text{F}_6$  complex. The  $\text{I}^-$  resides above the  $\text{C}_6\text{F}_6$  ring at a distance of 3.69 Å. The charge is almost exclusively on the iodide, as was also inferred from the experimental photoelectron spectra. To map the PES, the distance between the centroid of the ring and  $\text{I}^-$ ,  $R$ , was varied and the resulting energy calculated. The result of such a scan is shown in Figure 2(b) and (c) for the neutral and anionic complexes, respectively. As  $R \rightarrow \infty$ , the difference between the neutral and anion PES is simply the electron affinity of I. Our calculations yield an energy difference of 3.13 eV (at  $R = 30$  Å), very close to the known electron affinity, 3.06 eV. We have shifted the neutral surface so that it reproduces the correct value. All energies in Figure 2 are referenced to the minimum of the anion PES.

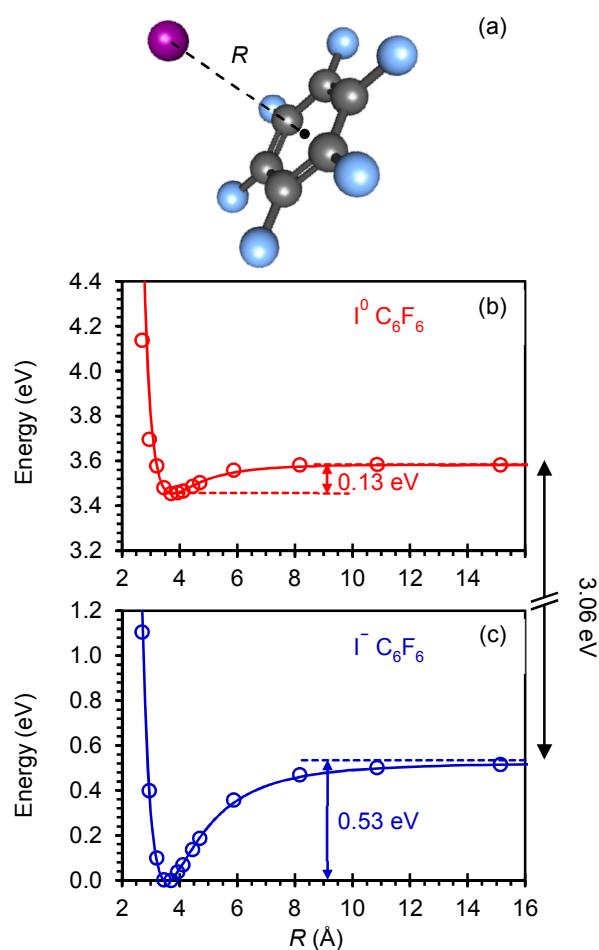
Figure 2(b) and (c) also includes fits to a Leonard-Jones potential,  $V_{\text{LJ}}$ , of the form:

$$V_{\text{LJ}}(R) = D_e \left[ \left( \frac{R_0}{R} \right)^{2n} - 2 \left( \frac{R_0}{R} \right)^n \right],$$

where  $\varepsilon$  is the dissociation energy,  $R_0$  is the internuclear distance at the minimum of the curve, and  $n$  is an index that provides a physical description of the interaction. The overall fit to the calculated energies for the anion is excellent. Deviations at small  $R$  arise because of the (well-known) incorrect description of the repulsive component in  $V_{\text{LJ}}(R)$ . For the anion- $\pi$  bond, the Leonard-Jones parameters are:  $D_e = 0.53$  eV,  $R_0 = 3.56$  Å; and  $n = 3.34$ . If the interaction were purely electrostatic charge-quadrupole in nature, then one would expect that  $n = 3$  (*i.e.*  $R^{-3}$  long-range dependence). The fitted  $R_0$  value is some way off the equilibrium 3.69 Å distance calculated in Figure 2(a). However, the potential is relatively flat and the energy difference at  $R = 3.45$  Å and 3.69 Å is only 2.5 meV.

The fit of the computed neutral PES to  $V_{\text{LJ}}(R)$  is slightly poorer (see Figure 2(b)), but we nevertheless included this to enable comparison. The Leonard-Jones parameters for the neutral complex are  $D_e = 0.13$  eV,  $R_0 = 3.76$  Å; and  $n = 4.35$ . The larger value for  $n$  is consistent with the loss of the charge.

Figure 2: (a) Minimum energy structure of  $\text{I}^-\text{C}_6\text{F}_6$  and potential energy curves for (b)  $\text{I}^0\text{C}_6\text{F}_6$  and (c)  $\text{I}^-\text{C}_6\text{F}_6$  as a function of separation between the I and the center of the  $\text{C}_6\text{F}_6$  ring. The solid lines



in (b) and (c) are Leonard-Jones potential energy functions with parameters defined in the text.

Interestingly, although the interaction in neutral complex is significantly weaker than in the anion,  $R_0$  has not changed by a large amount, especially given the flatness of the PES.

In photoelectron spectroscopy, it is the vertical difference in energy from the anion minimum to the neutral that is measured. From Figure 2, the computed energy difference at  $R_0 = 3.56$  Å is 0.40 eV, in excellent agreement with the measured  $\Delta\text{eBE} = 0.42 \pm 0.02$  eV. We thus conclude that the calculated PES for the anion and neutral are representative of the complexes and that the calculated anion PES describes the anion- $\pi$  bond accurately. The anion- $\pi$  bond dissociation,  $D_e = 0.53$  eV ( $51 \text{ kJ mol}^{-1}$ ). It is not possible to determine an accurate error for this value because it is in part derived from the computational work. However, given the overall agreement

between experiment and theory, the uncertainty is likely to be less than  $\pm 0.03$  eV.

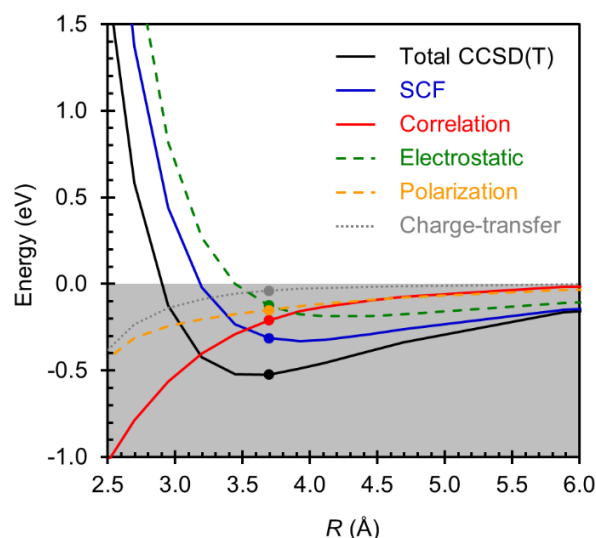


Figure 3: Contributions to the calculated total energy from the SCF and correlation energies. The SCF energy is further decomposed into contributions from electrostatic, polarization and charge-transfer interactions. The points indicate the decomposed energies at the calculated minimum energy geometry. The grey area indicates regions of attractive interactions.

In arriving at the anion- $\pi$  bond strength, a number of assumptions have been made. It is assumed that  $R$  is a unique coordinate and ignores the associated angular (*i.e.* bend) motion. However, the PES overall is very flat in this region and therefore, such motion is not likely to have a large impact on the result. We have also ignored the zero-point energy contribution of the anion- $\pi$  bond. A particularly useful aspect of  $V_{LJ}(R)$  is that the harmonic frequency of the vibration can be defined based on the parameters:

$$\nu_e = (n/2\pi R_0)(D_e/\mu)^{1/2},$$

where  $\mu$  is the reduced mass of  $\Gamma\text{-C}_6\text{F}_6$ . The (harmonic) zero-point energy of the anion- $\pi$  bond vibration is 2.5 meV ( $20\text{ cm}^{-1}$ ). Hence, the correction to  $\Delta e\text{BE}$  is very small. A further approximation made is that we have simply used the difference in energies between the PESs at the anion geometry and not calculated the Franck-Condon factors. However, given the relative flatness of the PESs, this also does not introduce a large error. By inspection of the anion PES, the turning points for the  $\nu = 0$  level are at  $R \sim 3.48$  and  $3.63$  Å. Vertical projection from these points to the neutral PES results in changes in the observable  $\Delta e\text{BE}$  of less than 0.01 eV. This insensitivity also accounts for similarity in width of the photoelectron spectra of  $\Gamma^-$  and  $\Gamma\text{-C}_6\text{F}_6$ .

Our results highlight that the key physical interactions are well-accounted for by the calculations. The calculations now also allow us to disentangle the dominant contributions to the total binding energy. In Figure 3, we show an analysis of the main contributions to the anion- $\pi$  bond. The SCF energy can be further decomposed into electrostatic, polarization and charge-transfer interactions using the ALMO-EDA approach. At the minimum energy geometry, the SCF binding is 0.31 eV, of which 0.12 eV is electrostatic, and 0.15 eV is due to polarization interactions (a further 0.04 from delocalization/charge-transfer). The purely electrostatic interaction

arises between the negative charge localized on  $\Gamma^-$  and the positive quadrupole-moment of  $\text{C}_6\text{F}_6$  ( $Q_{zz} = +9.50$  B). In terms of overall contributions to the total anion- $\pi$  binding, the relative ratio of electrostatic:polarization:correlation is 23:28:41 (at the calculated minimum energy geometry). Hence, while the positive quadrupole is an important driver for the anion- $\pi$  bond, the correlation energy is the dominant contributor, accounting for  $\sim 40\%$  of the total anion- $\pi$  bond strength. Correlation has been recognized as a key component to the interaction (even for electron binding<sup>28,36,37</sup>), but without spectroscopic data, the relative contribution has become a source of debate.<sup>38</sup>

Many previous experimental studies have focused on unravelling the interplay of anion- $\pi$  and other non-covalent interactions in the binding of anions to  $\pi$ -rich molecules, partly because it is often difficult to study pure anion- $\pi$  complexes.<sup>39</sup> However, the anion- $\pi$  bond as measured here is strong in its own right. We note that molecules with much larger  $Q_{zz}$  have been synthesized and with large  $\pi$ -systems for which electrostatic, polarization and correlation interaction will be even larger.<sup>40</sup> Also, the identity of the anion is important. For halides complexed to  $\text{C}_6\text{F}_6$ , computational studies have shown that the bond strength decreases with halide size so that the anion- $\pi$  in  $\Gamma\text{-C}_6\text{F}_6$  may be expected to be the weakest in the halide series.<sup>7,41</sup>

In conclusion, we have determined the anion- $\pi$  bond dissociation energy in  $\Gamma\text{-C}_6\text{F}_6$  to be 0.53 eV ( $51\text{ kJ mol}^{-1}$ ) using a combination of anion photoelectron spectroscopy and high-level electronic structure theory. The bond has a  $\sim 40\%$  correlation interaction contribution with the remaining arising from the electrostatic quadrupole-charge interaction ( $\sim 20\%$ ) and polarization ( $\sim 30\%$ ). To the best of our knowledge, this presents the first rigorous spectroscopic determination of an anion- $\pi$  bond energy. The strength of the interaction suggests that anion- $\pi$  bonds are important non-covalent interactions, even though they are often observed in competition with other non-covalent interactions. The use of anion photoelectron spectroscopy coupled with accurate electronic structure calculations is applicable to a wide host of anion- $\pi$  bonded complexes and paves the way to studying how competing effects alter the anion- $\pi$  bond.

## AUTHOR INFORMATION

### Corresponding Author

j.r.r.verlet@durham.ac.uk

### Notes

The authors declare no competing financial interests.

## ACKNOWLEDGMENT

We would like to thank Andrew Ellis (Leicester) for useful discussions. This work has been funded by the European Research Council under Starting Grant 306536.

## REFERENCES

- (1) Meyer, E. A.; Castellano, R. K.; Diederich, F. Interactions with Aromatic Rings in Chemical and Biological Recognition. *Angew. Chem. Int. Ed.* **2003**, *42* (11), 1210–1250.
- (2) Salonen, L. M.; Ellermann, M.; Diederich, F. Aromatic Rings in Chemical and Biological Recognition: Energetics and Structures. *Angew. Chem. Int. Ed.* **2011**, *50* (21), 4808–4842.
- (3) Schneider, H.-J. Binding Mechanisms in Supramolecular Complexes. *Angew. Chem. Int. Ed.* **2009**, *48* (22), 3924–3977.
- (4) Mecozzi, S.; West, A. P.; Dougherty, D. A. Cation- $\pi$  Interactions in Aromatics of Biological and Medicinal Interest: Electrostatic Potential Surfaces as a Useful Qualitative Guide. *Proc. Natl. Acad. Sci.* **1996**, *93* (20), 10566–10571.

- 1  
2  
3 (5) Wheeler, S. E.; Bloom, J. W. G. Toward a More Complete Understanding of Noncovalent Interactions Involving Aromatic Rings. *J. Phys. Chem. A* **2014**, *118* (32), 6133–6147.
- 4 (6) Hunter, C. A.; Sanders, J. K. M. The Nature of  $\pi$ - $\pi$  Interactions. *J. Am. Chem. Soc.* **1990**, *112* (14), 5525–5534.
- 5 (7) Quiñero, D.; Garau, C.; Rotger, C.; Frontera, A.; Ballester, P.; Costa, A.; Deyà, P. M. Anion- $\pi$  Interactions: Do They Exist? *Angew. Chem. Int. Ed.* **2002**, *41* (18), 3389–3392.
- 6 (8) Alkorta, I.; Rozas, I.; Elguero, J. Interaction of Anions with Perfluoro Aromatic Compounds. *J. Am. Chem. Soc.* **2002**, *124* (29), 8593–8598.
- 7 (9) Mascal, M.; Armstrong, A.; Bartberger, M. D. Anion-Aromatic Bonding: A Case for Anion Recognition by  $\pi$ -Acidic Rings. *J. Am. Chem. Soc.* **2002**, *124* (22), 6274–6276.
- 8 (10) Frontera, A.; Gamez, P.; Mascal, M.; Mooibroek, T. J.; Reedijk, J. Putting Anion- $\pi$  Interactions Into Perspective. *Angew. Chem. Int. Ed.* **2011**, *50* (41), 9564–9583.
- 9 (11) Garau, C.; Frontera, A.; Quiñero, D.; Ballester, P.; Costa, A.; Deyà, P. M. A Topological Analysis of the Electron Density in Anion- $\pi$  Interactions. *ChemPhysChem* **2003**, *4* (12), 1344–1348.
- 10 (12) Wang, D.-X.; Wang, M.-X. Anion- $\pi$  Interactions: Generality, Binding Strength, and Structure. *J. Am. Chem. Soc.* **2013**, *135* (2), 892–897.
- 11 (13) Zhao, Y.; Domoto, Y.; Orentas, E.; Beuchat, C.; Emery, D.; Mareda, J.; Sakai, N.; Matile, S. Catalysis with Anion- $\pi$  Interactions. *Angew. Chem. Int. Ed.* **2013**, *52* (38), 9940–9943.
- 12 (14) Giese, M.; Albrecht, M.; Rissanen, K. Experimental Investigation of Anion- $\pi$  Interactions – Applications and Biochemical Relevance. *Chem. Commun.* **2016**, *52* (9), 1778–1795.
- 13 (15) Chifotides, H. T.; Dunbar, K. R. Anion- $\pi$  Interactions in Supramolecular Architectures. *Acc. Chem. Res.* **2013**, *46* (4), 894–906.
- 14 (16) Schottel, B. L.; Chifotides, H. T.; Dunbar, K. R. Anion- $\pi$  Interactions. *Chem. Soc. Rev.* **2007**, *37* (1), 68–83.
- 15 (17) Guha, S.; Saha, S. Fluoride Ion Sensing by an Anion- $\pi$  Interaction. *J. Am. Chem. Soc.* **2010**, *132* (50), 17674–17677.
- 16 (18) Dawson, R. E.; Hennig, A.; Weimann, D. P.; Emery, D.; Ravikumar, V.; Montenegro, J.; Takeuchi, T.; Gabutti, S.; Mayor, M.; Mareda, J.; Schalley, C. A.; Matile, S. Experimental Evidence for the Functional Relevance of Anion- $\pi$  Interactions. *Nat. Chem.* **2010**, *2* (7), 533–538.
- 17 (19) Chakravarty, S.; Ung, A. R.; Moore, B.; Shore, J.; Alshamrani, M. A Comprehensive Analysis of Anion-Quadrupole Interactions in Protein Structures. *Biochemistry* **2018**, *57* (12), 1852–1867.
- 18 (20) Giese, M.; Albrecht, M.; Rissanen, K. Anion- $\pi$  Interactions with Fluoroarenes. *Chem. Rev.* **2015**, *115* (16), 8867–8895.
- 19 (21) Guha, S.; Goodson, F. S.; Corson, L. J.; Saha, S. Boundaries of Anion/Naphthalenediimide Interactions: From Anion- $\pi$  Interactions to Anion-Induced Charge-Transfer and Electron-Transfer Phenomena. *J. Am. Chem. Soc.* **2012**, *134* (33), 13679–13691.
- 20 (22) Ma, J. C.; Dougherty, D. A. The Cation- $\pi$  Interaction. *Chem. Rev.* **1997**, *97* (5), 1303–1324.
- 21 (23) Papp, D.; Rovó, P.; Jákli, I.; Császár, A. G.; Perczel, A. Four Faces of the Interaction between Ions and Aromatic Rings. *J. Comput. Chem.* **2017**, *38* (20), 1762–1773.
- 22 (24) Bauzá, A.; Quiñero, D.; Deyà, P. M.; Frontera, A. Quadrupole Moment versus Molecular Electrostatic Potential: Strange Behavior of Ethynyl-Substituted Benzenes. *Chem. Phys. Lett.* **2013**, *567*, 60–65.
- 23 (25) López-Andarias, J.; Bauzá, A.; Sakai, N.; Frontera, A.; Matile, S. Remote Control of Anion- $\pi$  Catalysis on Fullerene-Centered Catalytic Triads. *Angew. Chem.* **2018**, *130* (34), 11049–11053.
- 24 (26) Göth, M.; Witte, F.; Quennet, M.; Jungk, P.; Podolan, G.; Lentz, D.; Hoffmann, W.; Pagel, K.; Reissig, H.-U.; Paulus, B.; Schalley, C. A. To Anion- $\pi$  or Not to Anion- $\pi$ : The Case of Anion-Binding to Divalent Fluorinated Pyridines in the Gas Phase. *Chem. – Eur. J.* **2018**, *24* (49), 12879–12889.
- 25 (27) Zhang, J.; Zhou, B.; Sun, Z.-R.; Wang, X.-B. Photoelectron Spectroscopy and Theoretical Studies of Anion- $\pi$  Interactions: Binding Strength and Anion Specificity. *Phys. Chem. Chem. Phys.* **2015**, *17* (5), 3131–3141.
- 26 (28) Rogers, J. P.; Anstöter, C. S.; Verlet, J. R. R. Ultrafast Dynamics of Low-Energy Electron Attachment via a Non-Valence Correlation-Bound State. *Nat. Chem.* **2018**, *10* (3), 341–346.
- 27 (29) Rogers, J. P.; Anstöter, C. S.; Bull, J. N.; Curchod, B. F. E.; Verlet, J. R. R. Photoelectron Spectroscopy of the Hexafluorobenzene Cluster Anions: (C<sub>6</sub>F<sub>6</sub>)<sup>n-</sup> (n = 1–5) and I-(C<sub>6</sub>F<sub>6</sub>). *J. Phys. Chem. A* **2019**, *123* (8), 1602–1612.
- 28 (30) Eppink, A. T. J. B.; Parker, D. H. Velocity Map Imaging of Ions and Electrons Using Electrostatic Lenses: Application in Photoelectron and Photofragment Ion Imaging of Molecular Oxygen. *Rev. Sci. Instrum.* **1997**, *68* (9), 3477–3484.
- 29 (31) Roberts, G. M.; Nixon, J. L.; Lecointre, J.; Wrede, E.; Verlet, J. R. R. Toward Real-Time Charged-Particle Image Reconstruction Using Polar Onion-Peeling. *Rev. Sci. Instrum.* **2009**, *80* (5), 053104.
- 30 (32) Piecuch, P.; Wloch, M. Renormalized Coupled-Cluster Methods Exploiting Left Eigenstates of the Similarity-Transformed Hamiltonian. *J. Chem. Phys.* **2005**, *123* (22), 224105.
- 31 (33) Dunning, T. H. Gaussian Basis Sets for Use in Correlated Molecular Calculations. I. The Atoms Boron through Neon and Hydrogen. *J. Chem. Phys.* **1989**, *90* (2), 1007–1023.
- 32 (34) Shao, Y.; Gan, Z.; Epifanovsky, E.; Gilbert, A. T. B.; Wormit, M.; Kussmann, J.; Lange, A. W.; Behn, A.; Deng, J.; Feng, X.; Ghosh, D.; Goldey, M.; Horn, P. R.; Jacobson, L. D.; Kaliman, I.; Khalullin, R. Z.; Kuš, T.; Landau, A.; Liu, J.; Proynov, E. I.; Rhee, Y. M.; Richard, R. M.; Rohrdanz, M. A.; Steele, R. P.; Sundstrom, E. J.; III, H. L. W.; Zimmerman, P. M.; Zuev, D.; Albrecht, B.; Alguire, E.; Austin, B.; Beran, G. J. O.; Bernard, Y. A.; Berquist, E.; Brandhorst, K.; Bravaya, K. B.; Brown, S. T.; Casanova, D.; Chang, C.-M.; Chen, Y.; Chien, S. H.; Closser, K. D.; Crittenden, D. L.; Diedenhofen, M.; Jr, R. A. D.; Do, H.; Dutoi, A. D.; Edgar, R. G.; Fatehi, S.; Fusti-Molnar, L.; Ghysels, A.; Golubeva-Zadorozhnaya, A.; Gomes, J.; Hanson-Heine, M. W. D.; Harbach, P. H. P.; Hauser, A. W.; Hohenstein, E. G.; Holden, Z. C.; Jagau, T.-C.; Ji, H.; Kaduk, B.; Khistyayev, K.; Kim, J.; Kim, J.; King, R. A.; Klunzinger, P.; Kosonen, D.; Kowalczyk, T.; Krauter, C. M.; Lao, K. U.; Laurent, A. D.; Lawler, K. V.; Levchenko, S. V.; Lin, C. Y.; Liu, F.; Livshits, E.; Lochan, R. C.; Luenser, A.; Manohar, P.; Manzer, S. F.; Mao, S.-P.; Mardirossian, L.; Marenich, A. V.; Maurer, S. A.; Mayhall, N. J.; Neuscammer, E.; Oana, C. M.; Olivares-Amaya, R.; O'Neill, D. P.; Parkhill, J. A.; Perrine, T. M.; Peverati, R.; Prociuk, A.; Rehn, D. R.; Rosta, E.; Russ, N. J.; Sharada, S. M.; Sharma, S.; Small, D. W.; Sodt, A.; Stein, T.; Stück, D.; Su, Y.-C.; Thom, A. J. W.; Tsuchimochi, T.; Vanovschi, V.; Vogt, L.; Vydrov, O.; Wang, T.; Watson, M. A.; Wenzel, J.; White, A.; Williams, C. F.; Yang, J.; Yeganeh, S.; Yost, S. R.; You, Z.-Q.; Zhang, I. Y.; Zhang, X.; Zhao, Y.; Brooks, B. R.; Chan, G. K. L.; Chipman, D. M.; Cramer, C. J.; III, W. A. G.; Gordon, M. S.; Hehre, W. J.; Klamt, A.; III, H. F. S.; Schmidt, M. W.; Sherrill, C. D.; Truhlar, D. G.; Warshel, A.; Xu, X.; Aspuru-Guzik, A.; Baer, R.; Bell, A. T.; Besley, N. A.; Chai, J.-D.; Dreuw, A.; Dunietz, B. D.; Furlani, T. R.; Gwaltney, S. R.; Hsu, C.-P.; Jung, Y.; Kong, J.; Lambrecht, D. S.; Liang, W.; Ochsenfeld, C.; Rassolov, V. A.; Slipchenko, L. V.; Subotnik, J. E.; Voorhis, T. V.; Herbert, J. M.; Krylov, A. I.; Gill, P. M. W.; Head-Gordon, M. Advances in Molecular Quantum Chemistry Contained in the Q-Chem 4 Program Package. *Mol. Phys.* **2015**, *113* (2), 184–215.
- 33 (35) Khalullin, R. Z.; Cobar, E. A.; Lochan, R. C.; Bell, A. T.; Head-Gordon, M. Unravelling the Origin of Intermolecular Interactions Using Absolutely Localized Molecular Orbitals. *J. Phys. Chem. A* **2007**, *111* (36), 8753–8765.
- 34 (36) Bull, J. N.; Verlet, J. R. R. Observation and Ultrafast Dynamics of a Nonvalence Correlation-Bound State of an Anion. *Sci. Adv.* **2017**, *3* (5), e1603106.
- 35 (37) Rogers, J. P.; Anstöter, C. S.; Verlet, J. R. R. Evidence of Electron Capture of an Outgoing Photoelectron Wave by a Nonvalence State in (C<sub>6</sub>F<sub>6</sub>)<sup>n-</sup>. *J. Phys. Chem. Lett.* **2018**, *9* (10), 2504–2509.
- 36 (38) Wheeler, S. E.; Houk, K. N. Are Anion/ $\pi$  Interactions Actually a Case of Simple Charge-Dipole Interactions? *J. Phys. Chem. A* **2010**, *114* (33), 8658–8664.
- 37 (39) Bornhof, A.-B.; Bauzá, A.; Aster, A.; Pupier, M.; Frontera, A.; Vauthey, E.; Sakai, N.; Matile, S. Synergistic Anion-( $\pi$ )<sub>n</sub>- $\pi$  Catalysis on  $\pi$ -Stacked Foldamers. *J. Am. Chem. Soc.* **2018**, *140* (14), 4884–4892.
- 38 (40) Wang, C.; Miros, F. N.; Mareda, J.; Sakai, N.; Matile, S. Asymmetric Anion- $\pi$  Catalysis on Perylenediimides. *Angew. Chem. Int. Ed.* **2016**, *55* (46), 14422–14426.
- 39 (41) Mezei, P. D.; Csonka, G. I.; Ruzsinszky, A.; Sun, J. Accurate, Precise, and Efficient Theoretical Methods To Calculate Anion- $\pi$

1  
2  
3  
4  
5  
6  
7  
8  
9  
10  
11  
12  
13  
14  
15  
16  
17  
18  
19  
20  
21  
22  
23  
24  
25  
26  
27  
28  
29  
30  
31  
32  
33  
34  
35  
36  
37  
38  
39  
40  
41  
42  
43  
44  
45  
46  
47  
48  
49  
50  
51  
52  
53  
54  
55  
56  
57  
58  
59  
60

Interaction Energies in Model Structures. *J. Chem. Theory Comput.* **2015**, *11* (1), 360–371.

1  
2  
3  
4  
5  
6  
7  
8  
9  
10  
11  
12  
13  
14  
15  
16  
17  
18  
19  
20  
21  
22  
23  
24  
25  
26  
27  
28  
29  
30  
31  
32  
33  
34  
35  
36  
37  
38  
39  
40  
41  
42  
43  
44  
45  
46  
47  
48  
49  
50  
51  
52  
53  
54  
55  
56  
57  
58  
59  
60

---

Graphic entry for the Table of Contents (TOC):

